ENERGY EFFICIENT METHOD FOR ENERGY RECOVERY FROM BIOGAS PRODUCTION

Janis Ratnieks[1,2], Andris Jakovics[1], Reviks Vardanjans[2], Aigars Laizans[3], Davids Vardanjans[2]

[1]University of Latvia, Faculty of physics and mathematics, Zellu street 8, Riga, Latvia

[2]Armgate Ltd., Liliju street 20, Marupe, Latvia

[3]Latvian University of Agriculture, Institute of Power Energetics, J.Cakstes boulevard 5, Jelgava, Latvia

Abstract

A new method for biogas heating, cooling and drying has been developed. The method is based on two channel counter flow where recuperation happens. Biogas cooling is done with the dried colder flow to get the gas below the dew point temperature and allow it to condensate, but heating is done with humid hot gas flow from bioreactor. The system is being tested both experimentally and numerically by mathematical modelling. A previously developed 1D model has been implemented in MATLAB and calculations made for experimental setup. The results are also compared to 3D model made with ANSYS/CFX software.

Keywords: *Experimental verification, mathematical modelling, counter flow, bioreactor*

1. INTRODUCTION

To increase the bioreactor performance a method of two channel counter flow is being suggested. The main idea of the system is that of a heat exchanger where hot gas heats the cold one and the cold one is used to cool the hot one. A double layer system is being proposed that is mounted around the reactor walls, a schematic picture of the bioreactor and the counter flow channel structure are provided in figure 1.

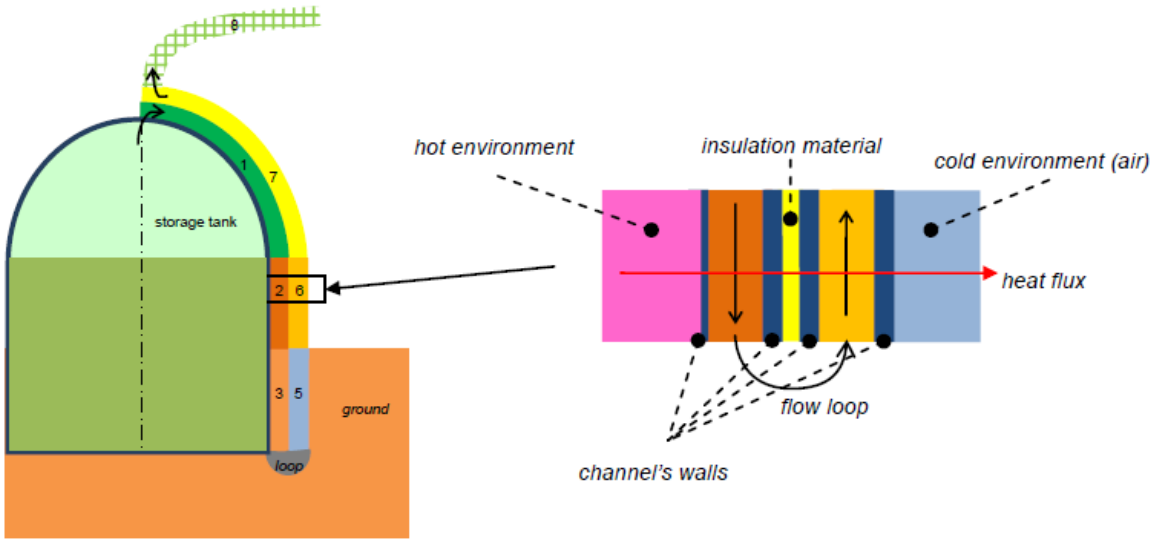


Figure 1: Schematic picture of heat exchange system being developed

A mathematical model for temperature in 1D case has been developed by (Jakovics, et al., 2014). The general assumptions for the model as well as governing equations are given in chapter 2. An experiment has been made to check the mathematical model for the case when only channels, 2 and 6

as well as the loop is present (see Fig. 1), the experimental setup is described in detail in chapter 3. Additionally, a 3D model has been made in commercial package *ANSYS/CFX* and calculations done for experimental case, to see the effects that can't be predicted by 1D model.

2. MATHEMATICAL MODELS

2.1. 1D model

The channel length, no matter what is its actual spatial placement, is denoted by x. As we need to find out the temperature along the channel length, the variable solved for is temperature – T, see figure 2a. For the general case there is a heat flux through all the channel walls (fig. 2b), but due to symmetry, it is assumed that there is no heat flux between nearby channels with the same flow direction, see figure 2c. There is a heat flux between counter flow channels, reactor and outside environment, see figure 2c.

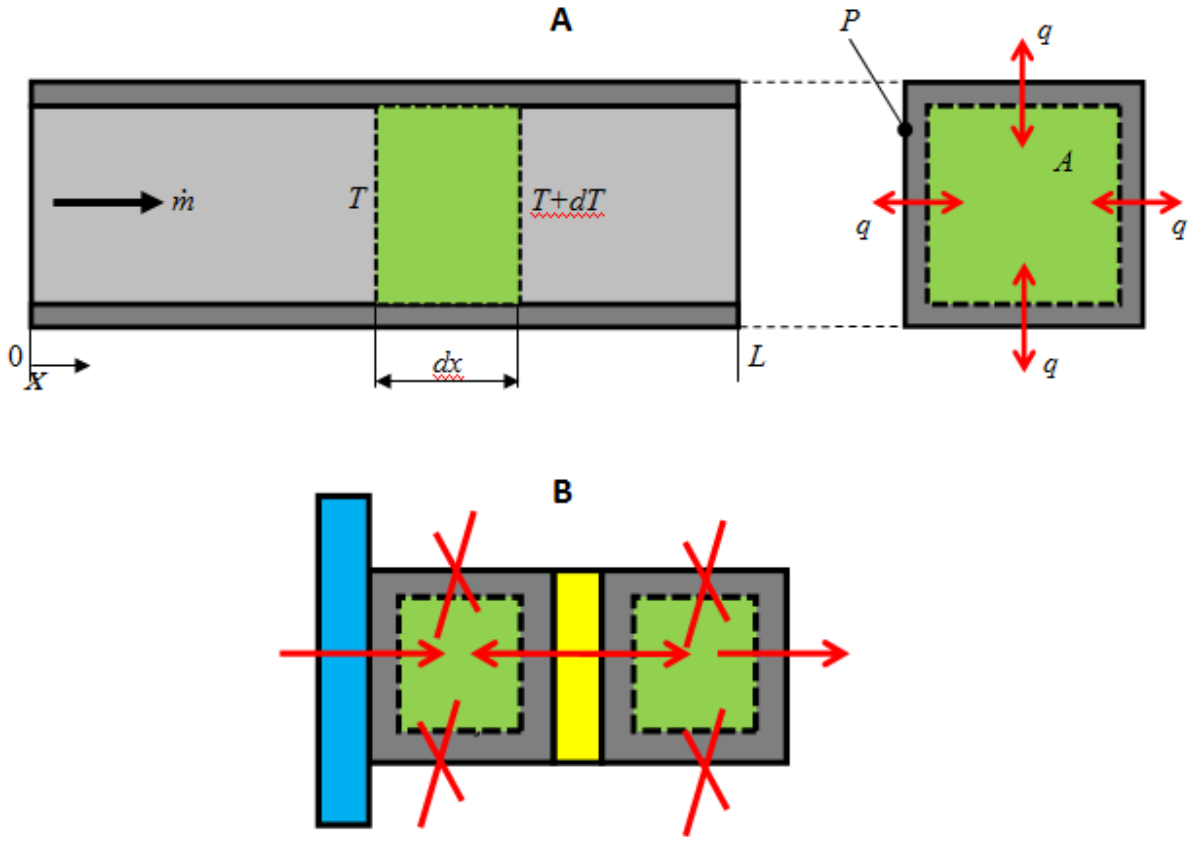


Figure 2: Schematic picture of a) channel cross sections b) channel system cross section with assumed heat fluxes.

If the heat capacity and gas composition is constant, the change of heat power for small length *dx* can be written as (1), where: *c* – heat capacity at constant volume *[J/kgK]*, *m* – mass flux *[kg/s]*, *Q* – heat power *[W]* (Incopera, et al., 2011).

$$dQ = \dot{m}\, c\, \left[\left(T + dT\right) - T\right] = \dot{m}\, c\, dT \tag{1}$$

The heat power through the outer walls can be written as (2), where *P* – perimeter *[m]*

$$dQ = q\, P\, dx \tag{2}$$

The heat flux for a simple case when the outer temperature is constant can be described by Newton's law, where T_∞ – outside temperature *[C]*, $\bar{U}$ – heat transmittance coefficient *[W/m2K]*

$$q = \bar{U}\left(T_\infty - T\right) \tag{3}$$

Combining equations 1-3 one can get equations for temperature along channel.

$$\frac{dT}{dx} = \frac{P}{\dot{m}\, c}\bar{U}\Delta T \tag{4}$$

The outside temperature however is not constant and therefore the right hand side of (4) must be modified to take into account different outside temperatures for various sides of the channel. Furthermore, the temperatures in one section influence the temperature of another and therefore, they must be coupled. This fact makes the problem non linear and more difficult to solve. The eq. 4 is recast as:

$$\frac{dT}{dx} = \frac{1}{\dot{m}\, c}\left[P^*\ \bar{U}^*\ \left(T^*{}_\infty - T\right) + P^{\Delta x}\ \bar{U}^{\Delta x}\ \left(T_\infty\left(x+\Delta x\right) - T\right)\right] \tag{5}$$

where * indicates the constant outside temperature wall and Δx refers to coupled wall segments.

The coupling is schematically shown in Fig. 3 where all the sections are shown, however in this case only sections 2 and 6 is needed, see Fig. 1. To solve this non linear problem numerically, a MATLAB code is developed that uses Runge-Kutta fourth order method (Lindfield & Penny, 2012).

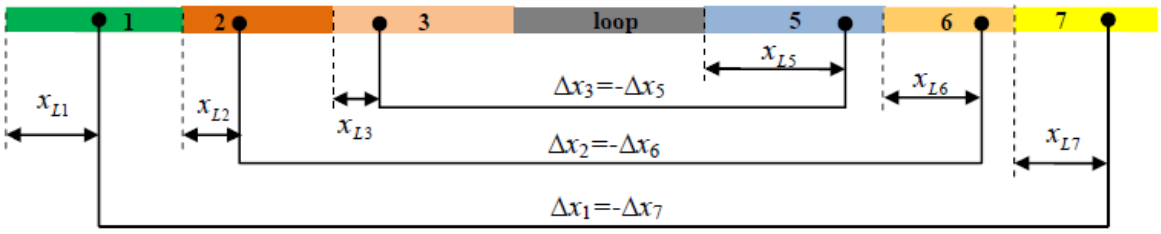


Figure 3: Schematic view of channel coupling.

The parameter values as well as inlet temperature for calculations are taken from the experiment and are given in chapter 3.

2.2. 3D model

As previously, it is assumed that heat flux is only between counter flows and only one coupled element represents the whole system, see Fig. 4

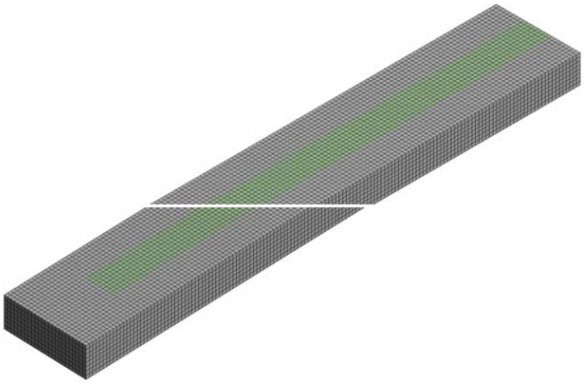


Figure 4: A 3D model with mesh.

Reynolds averaged Navier Stokes equation is being solved with *k-ω shear stress transport* turbulence model. The chosen turbulence model works well with laminar flows and therefore shouldn't give any meaningful differences. The flow is considered incompressible and Boussinesq approximation is used for buoyancy. The equations are well known and can be found in many standard texts on fluid mechanics (Versteeg & Malalasekera, 1995). The implementation in ANSYS/CFX can be found in (Ansys Inc, 2013)

There are third type boundary conditions for the hot and cold side for the temperature, the heat transfer coefficients that are calculated form thermal resistances. The outside and inlet temperature is taken from the experiment. For the flow there are no slip walls except for the inflow where the velocity is defined and outlet with 0 relative pressure.

3. EXPERIMENTAL SETUP

As we are only interested in bioreactor walls, the reactor itself is not necessary for the experiment. What matters is that the temperature of the wall surroundings is kept constant; therefore the wall was mounted in an old U-value measurement unit, where such conditions could be maintained, see Fig. 5.



Figure 5: Experimental setup

The wall itself, see figure 6, consists of two polycarbonate layers (heat exchangers) with an insulation layer between them, heater which provide constant temperature with a help of PID algorithm and wall imitation between the inner heat exchanger and heater. One channel is square with 1 cm edge length. The overall wall dimensions are 0.5 m horizontal time 1 m vertical direction.

In bioreactor there are gas mixture that consists of oxygen, nitrogen, water vapour, carbon dioxide and methane. The weighted average density is 1.606 kg/m^3 and heat capacity of 1787 J/kgK, in experiment however it is only air and water vapour and values of density 1.8 kg/m^3 and heat capacity of 1005 J/kgK are taken into account in calculations.

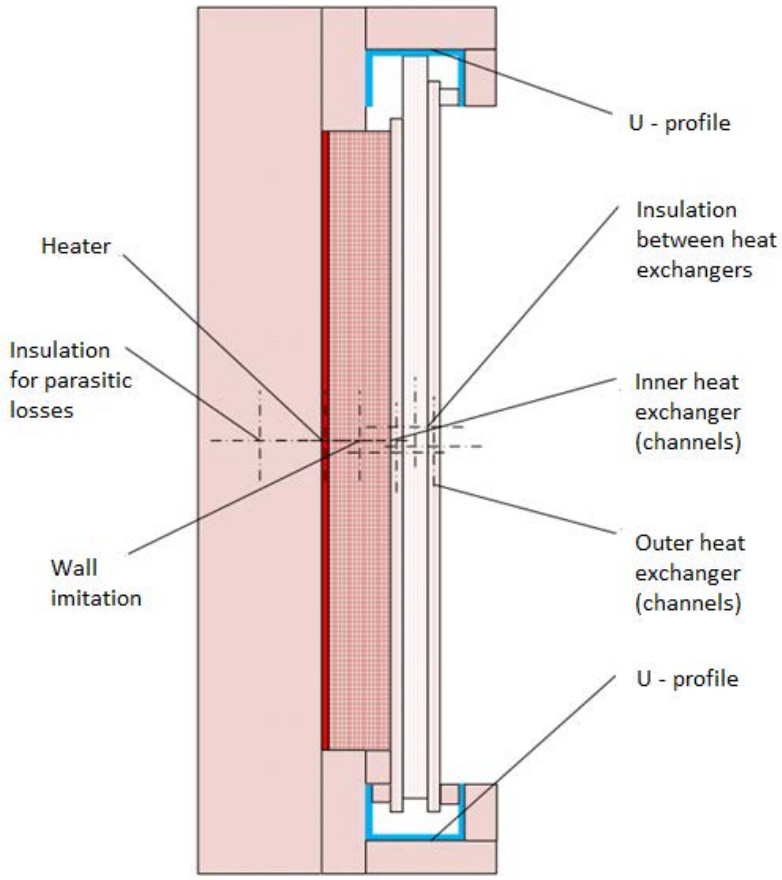


Figure 6: Schematic view of experimental setup

Temperature, humidity and heat flux sensors were mounted to acquire the experimental data. As the humidity is beyond the scope of this work, only the temperature sensor distribution is given:

- Heater,
- Between wall imitation and inner channel (*hot wall*),
- Between inner channel and insulation (*channel-isol hot side*),
- Between outer channel and insulation (*channel-isol cold side*),
- On outer channel surface (*ouside wall*),
- Cold room temperature (o*utside temperature*),
- Inflow
- Outflow
- Channel conjunction

Table 1: experimental setup

Case nr.	Heater temperature °C	Flow, l/min (cm/s)	Outside temperature, °C
1	38	12 (4)	22.6
2	38	10 (3.3)	22.4
3	32	10 (3.3)	14.1

4. RESULTS

It took a long time for experimental results to acquire stationary values, time dependence is shown in Figs. 7-9 and it can be seen that not all the values have achieved the stationary values. The given setup was held for 36 hours and for heat transmittance only the values should have become quasi stationary.

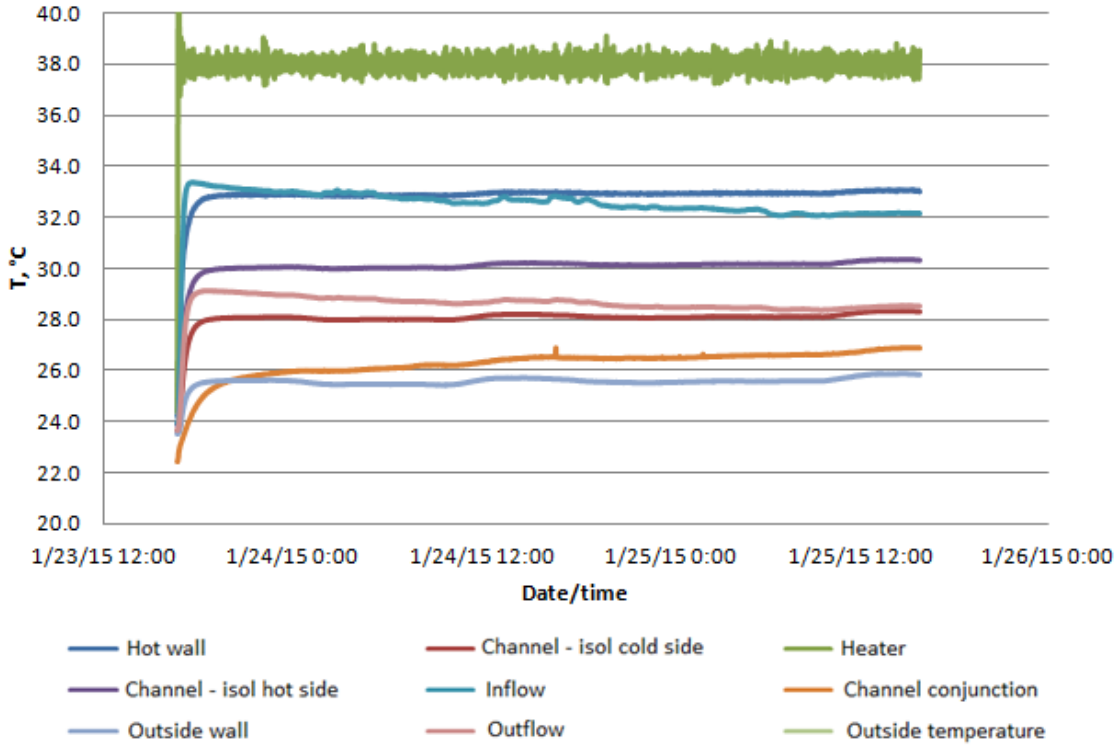


Figure 7: Temperature dependence on time for experimental setup 1.

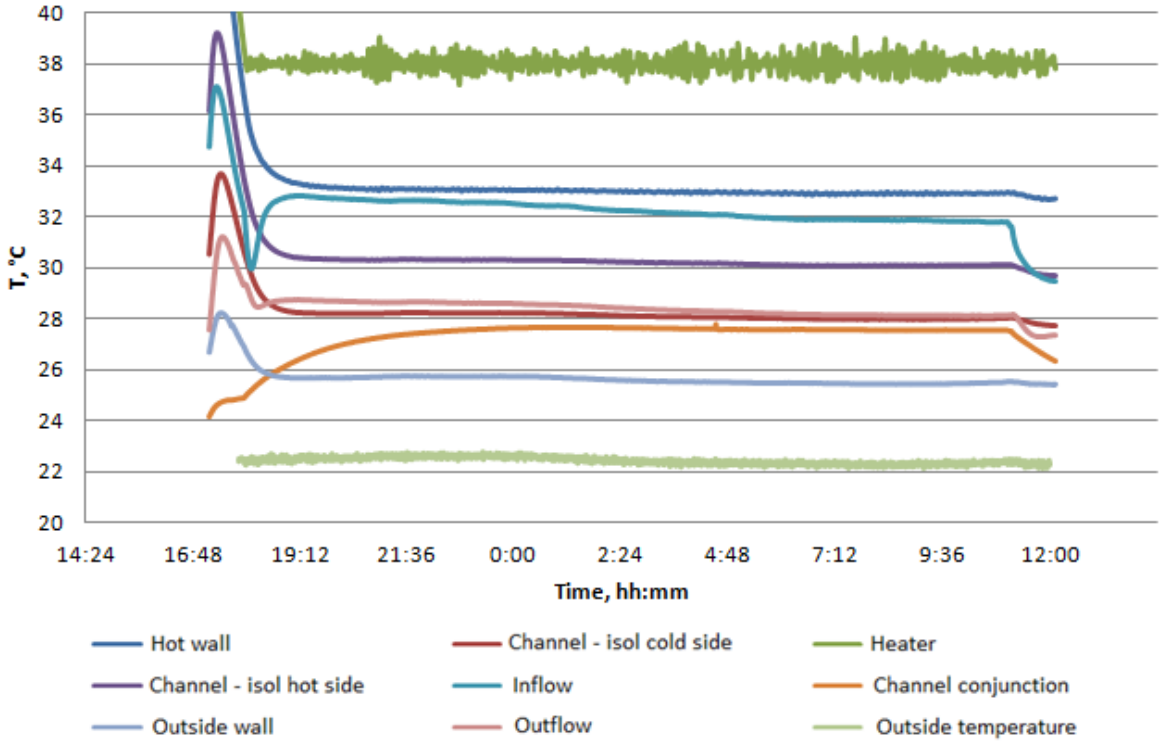


Figure 8: Temperature dependence on time for experimental setup 2.

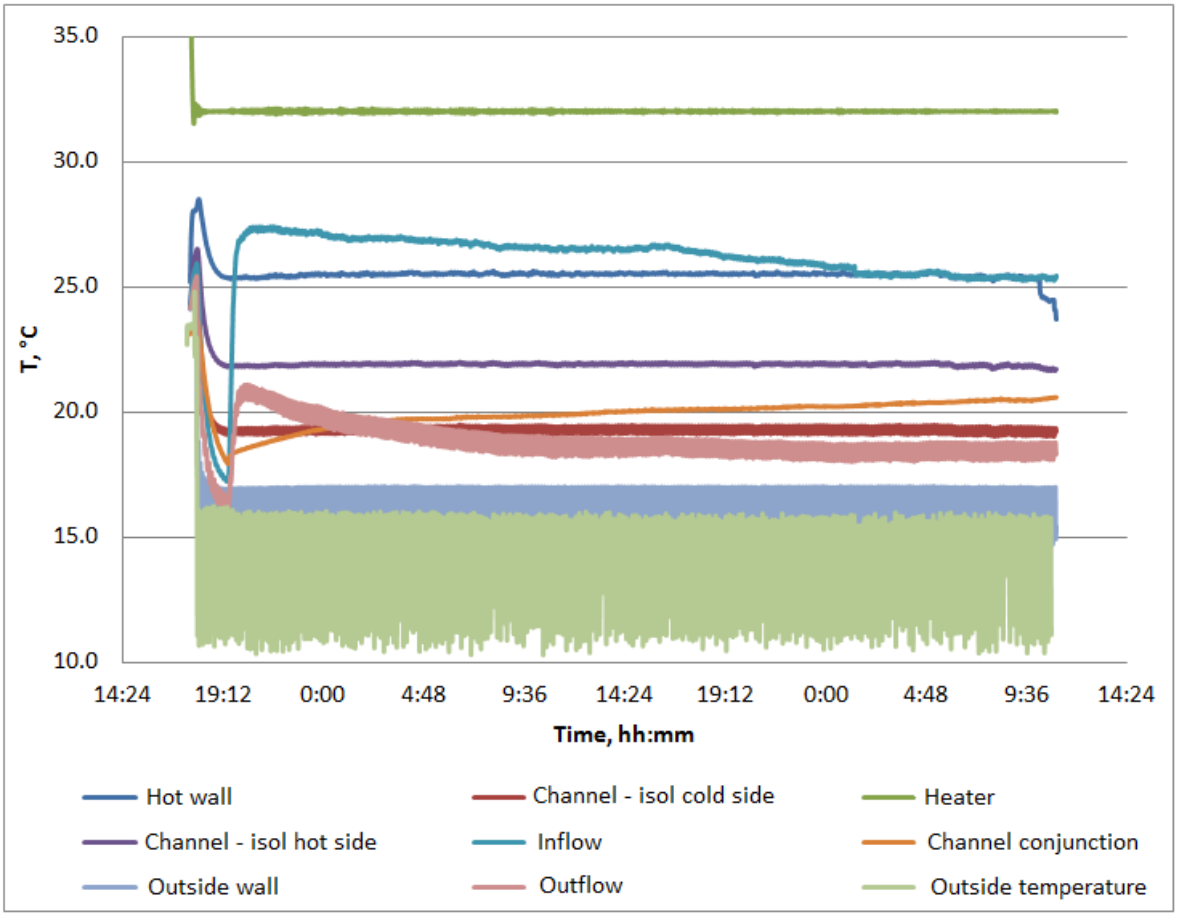


Figure 9: Temperature dependence on time for experimental setup 3.

The experimental inflow temperatures were given as boundary conditions for 1D simulation. The simulations were done for different thermal resistances and the results are shown in Table 2. Typical temperature distribution can be seen in Fig. 8 for boundary layer thermal resistance of 0.04 m^2K/W. After the fact that simulation outlet temperatures were lower than experimental, additional calculations for lower thermal resistance of insulation layer between channels were also carried out. This was done to see how the insulation affect the outlet temperature, because it is possible that in real measurement the insulation layer is a little bit pressed and therefore can have lower thermal resistance. It can be seen that two times lower thermal resistance rise the temperature for almost one degree Celsius, so one of the possible causes are the insulation layer. Another cause that is more plausible is that there is a thermal bridge because of U profile that is used in the construction of experiment.

Another interesting result is that the outlet temperatures do not change for various inlet velocities, the experimental data from cases one and two. The temperature difference is only 0.2° *C*, that is precision limit of the temperature sensors. Also the average outside temperature was 0.2° *C* higher for the higher outflow temperature.

Table 2: Simulation results for 1D case.

Inflow temperature, °C				25.4
Outside temperature, °C				14.1
Nr.	Inflow velocity	Boundary layer thermal resistance, m^2K/W	Insulation layer thermal resistance, m^2K/W	Outlet temperature, °C
1	3.3	0.02	0.2	16.2
2	3.3	0.04	0.2	16.7
3	3.3	0.06	0.2	17
4	1.65	0.04	0.2	16.7
5	4.95	0.04	0.2	16.7
6	6.6	0.04	0.2	16.7
7	3.3	0.04	0.1	18.6

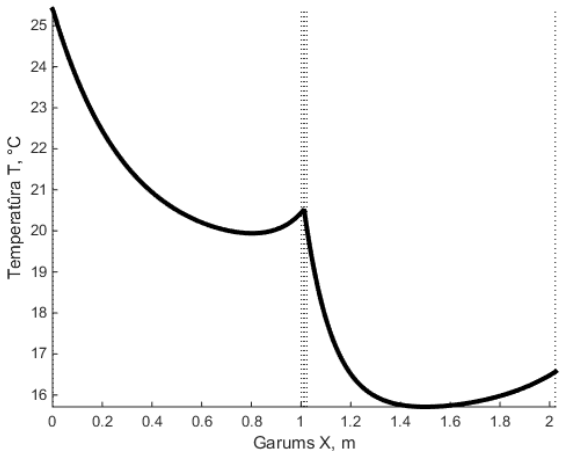


Figure 10: Temperature distribution along channel length for inflow velocity 3.3 *cm/s* and thermal resistance 0.04 m^2K/W

3D simulations were carried out to find out more about flow and possible 1D model issues. The results for different boundary layer values and different inflow velocities were carried out and the results are shown if Figs. 11 and 12 for thermal resistance and velocity sweeps respectively. The 3D results show qualitatively similar results as the 1 D model for different boundary layer thermal resistivity values. The higher is resistivity, the higher the outlet air temperature, however the absolute values are approximately a degree Celsius higher for 3D case then the 1D case. The temperature decrease more rapidly in 1D case in the inner channel and gets to values as low as 20° *C* that is the only major difference. The velocity sweep in 3D case shows that the outlet temperature is independent on the flow velocity in the range of application.

The average of temperatures for inner channel walls in experiment agrees well with air temperature in the middle of channel (where the sensors were placed) for 3D calculations. For the boundary layer thermal resistance 0.04 m^2K/W, inner channel temperatures for experiment and 3D simulation were 23.3° *C* and 22.7° C respectively and for outer channel 17.2° *C* and 17.1° *C*. The air outlet temperature difference is significant that means there is an additional heating in experiment that correspond to hypotheses that the U profile works as a thermal bridge.

As it can be seen in Figs. 13 and 14, the gravity makes the flow in the channel non uniform. In the inner channel there are greater velocities on the cold side, because the flow goes downwards and the gravity makes the cold air move faster. On the outer channel the effect is opposite as the gravity pushes the cold air downwards and therefore the flow upwards is slower at the colder side. This must be taken into account for boundary layer thermal resistances for 1D case. This however isn't be the main reason for that great difference in both models and 1D model has to be improved.

The temperature distribution in channel conjunction vary significantly depending on inlet velocity, this is because there is a backflow forming for low velocities that disappear at high velocities. The temperature sensor itself can considerably change the flow and temperatures in the region and therefore this is not taken into account. As it can be seen in Fig. 12, the temperature values for 3.3 *cm/s* flow that is also in the experiment, the temperature fluctuation there change in 2° *C* range.

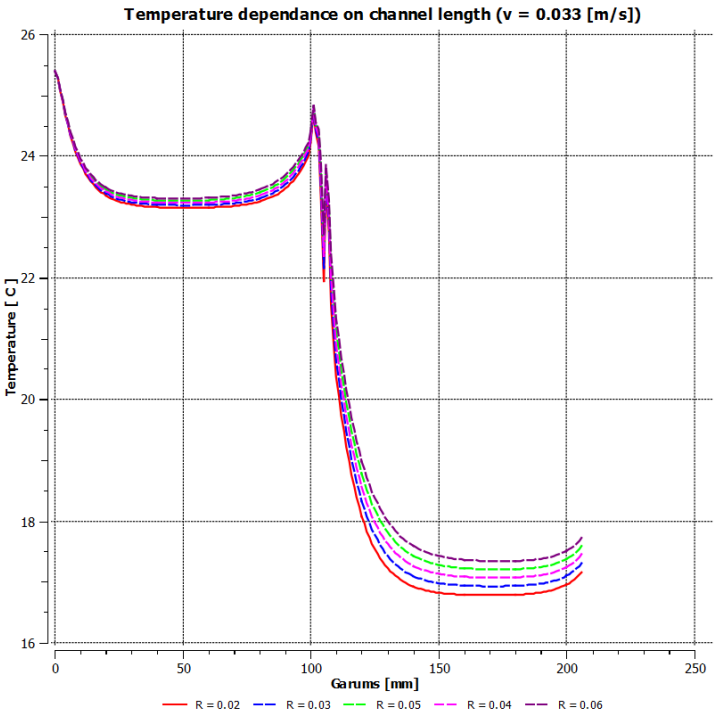


Figure 11: Temperature dependence on channel length for different thermal resistivity values and inlet velocity of 3.3 *cm/s*.

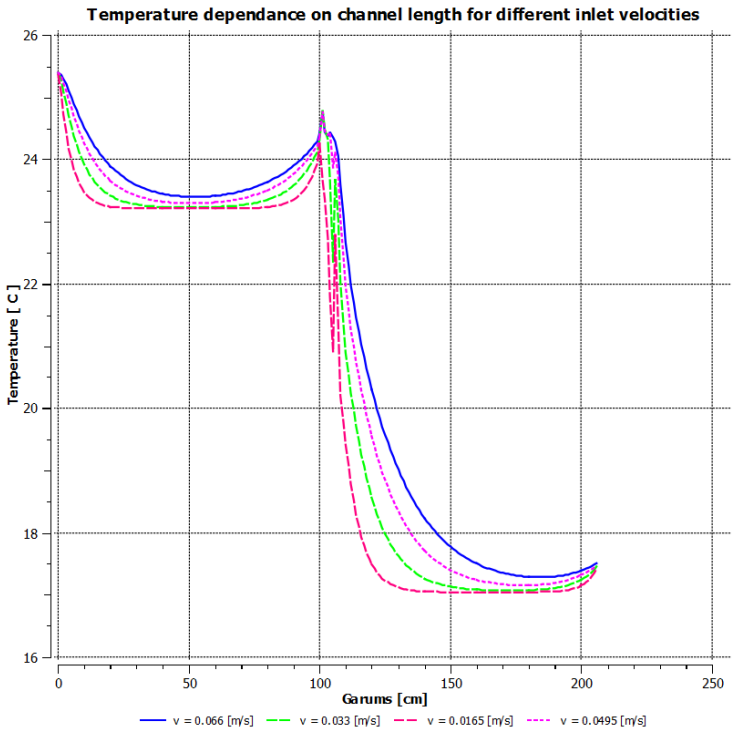


Figure 12: Temperature dependence on channel length for different inlet velocities and boundary layer thermal resistance of 0.04 m^2K/W for outside.

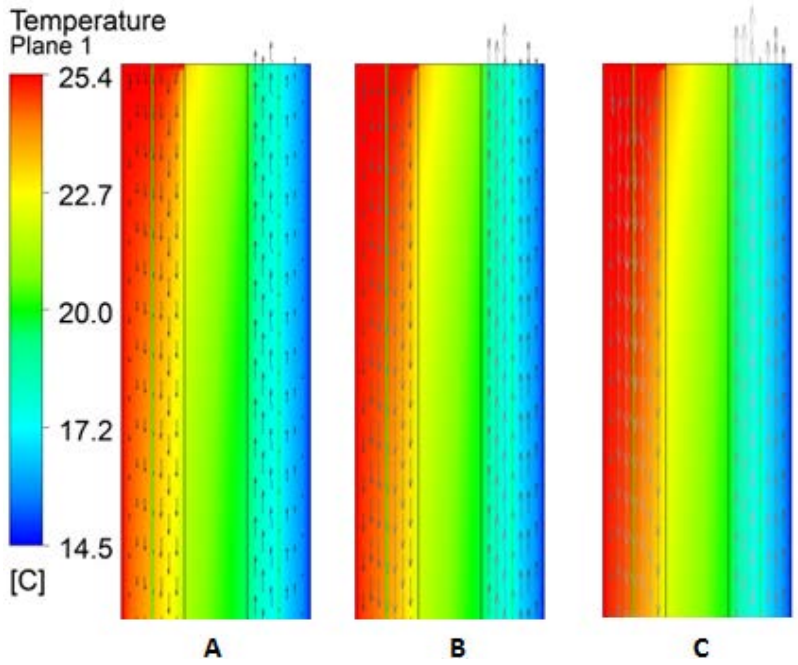


Figure 13: Temperature and air velocity vectors in the middle plane for inlet velocities a) 1.65 *cm/s* b) 3.3 *cm/s* c) 4.95 *cm/s*

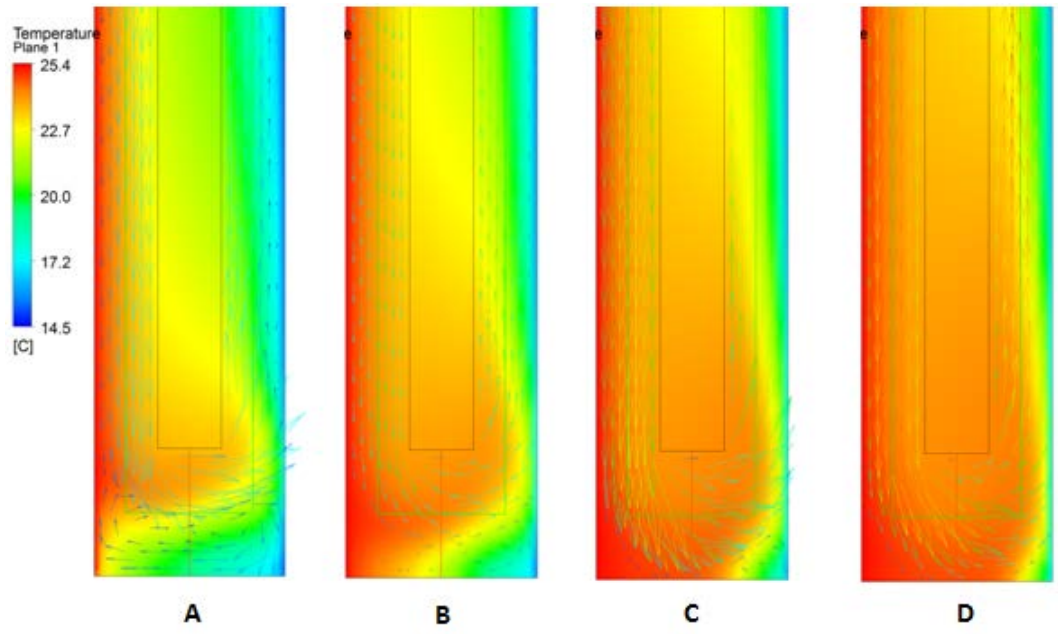


Figure 14: Temperature and air velocity for channel conjunction for different inlet velocities and thermal resistance of 0.04 m^2K/W a) v=1.65 *cm/s* b) v=3.3 *cm/s* c) v=4.95 *cm/s* d) v=6.6 *cm/s*

5. CONCLUSION

A qualitatively good agreement between the 3D model and experiment is achieved, the main reason that experimentally the outlet temperature is higher most likely is because of experimental setup and thermal bridge made by U profile. The 1D case however produces significantly different results and therefore the model must be revised. The future work will concentrate on better experimental setup by eliminating the thermal bridges. Another important thing that must be included in model is humidity and water condensate that should also be measured quantitatively in experiment. After the experimental setup was partly dismantled, the condensate was visible and therefore there is a good reason to believe that such technique should work for energy efficient drying of biogas.

ACKNOWLEDGEMENTS

This project is supported by cohesion fund, project nr. L-KL-11-0005

REFERENCES

Ansys Inc, 2013. *Ansys CFX User guide.* bez viet.:Ansys Inc..

Incopera, F., DeWitt, D., Bergman, T. & Lavine, A., 2011. *Fundamentals of heat and mass transfer.* 7th edition red. New York: John Wiley & Sons.

Jakovics, A., Gendelis, S., Laizans, A. & Vardanjans, D., 2014. Modelling of heat exchange in counterflow shell-type system. *(not published yet).*

Lindfield, G. & Penny, J., 2012. *Numerical methods using MATLAB.* Amsterdam: Academic Press.

Versteeg, H. & Malalasekera, W., 1995. *An Introduction to Computational Fluid Dynamics. The Finite Volume Method.* ISBN 0 582 21884 5 red. bez viet.:Longman Group Ltd..